Supplemental Data

Degradation-Mediated Protein

Quality Control in the Nucleus

Richard G. Gardner, Zara W. Nelson, and Daniel E. Gottschling

Supplemental Experimental Procedures

Microscopy

Fixation and DAPI-staining of cells was performed as previously described (Biggins et al., 1999). Cells expressing San1p-GFP fusion proteins were visualized on a Nikon Eclipse E600 microscope (Nikon Inc., Melville, NY) equipped with a 60X oil immersion objective and a 100 W mercury lamp. Filter sets to visualize GFP (HQ:FITC) and DAPI (UV-2E/C) were from Chroma Technology Corp (Brattleboro, Vermont). Images were captured with a Photometrics CoolSNAP fx, 12-bit, cooled CCD camera (Roper Scientific, Tucson, Arizona) and the accompanying RS Image software on an Apple Power Mac G4 (Apple Computer Inc., Cupertino, California).

Phenotypic Growth Assays

Growth assays were performed using various physical and chemical stresses. Heat sensitivity was assayed at 30˚C, 37˚C, and 39˚C on YEPD or YC plates. Hydrogen peroxide sensitivity was assayed on YC plates containing 0.005–0.5% H_2O_2. Canavanine sensitivity was assayed on YC plates containing 0.1–10µg/ml canavanine. $CdCl_2$ sensitivity was assayed on YC plates containing 0.05–0.3M $CdCl_2$. MMS and EMS sensitivities were assayed on YEPD plates containing 0.01–0.3% MMS or EMS. UV sensitivity was assayed by plating 400–600 cells onto YEPD plates and exposing the plates to 20–120 J/m^2 UV.

Supplemetnal References

Biggins, S., Severin, F.F., Bhalla, N., Sassoon, I., Hyman, A.A., and Murray, A.W. (1999). The conserved protein kinase Ipl1 regulates microtubule binding to kinetochores in budding yeast. Genes Dev. *13*, 532–544.

Brachmann, C.B., Davies, A., Cost, G. J., Caputo, E., Li, J., Hieter, P., and Boeke, J.D. (1998). Designer deletion strains derived from Saccharomyces cerevisiae S288C: a useful set of strains and plasmids for PCR-mediated gene disruption and other applications. Yeast *14*, 115–132.

Hughes, T.R., Weilbaecher, R.G., Walterscheid, M., and Lundblad, V. (2000). Identification of the single-strand telomeric DNA binding domain of the Saccharomyces cerevisiae Cdc13 protein. Proc. Natl. Acad. Sci. USA *97*, 6457–6462.

Peterson, S.E., Stellwagen, A.E., Diede, S.J., Singer, M.S., Haimberger, Z.W., Johnson, C.O., Tzoneva, M., and Gottschling, D.E. (2001). The function of a stem-loop in telomerase RNA is linked to the DNA repair protein Ku. Nat. Genet. *27*, 64–67.

Qi, H., and Zakian, V.A. (2000). The Saccharomyces telomere-binding protein Cdc13p interacts with both the catalytic subunit of DNA polymerase alpha and the telomerase-associated est1 protein. Genes Dev. *14*, 1777–1788.

Sikorski, R.S., and Hieter, P. (1989). A system of shuttle vectors and yeast host strains designed for efficient manipulation of DNA in Saccharomyces cerevisiae. Genetics *122*, 19–27.

Singer, M.S., and Gottschling, D. E. (1994). TLC1: template RNA component of Saccharomyces cerevisiae telomerase. Science *266*, 404–409.

Singer, M.S., Kahana, A., Wolf, A.J., Meisinger, L.L., Peterson, S.E., Goggin, C., Mahowald, M., and Gottschling, D.E. (1998). Identification of high-copy disruptors of telomeric silencing in Saccharomyces cerevisiae. Genetics *150*, 613–632.
Stone, E.M., Reifsnyder, C., McVey, M., Gazo, B., and Pillus, L. (2000). Two classes of sir3 mutants enhance the sir1 mutant mating defect and abolish telomeric silencing in Saccharomyces cerevisiae. Genetics *155*, 509–522.
Tong, A.H., Evangelista, M., Parsons, A.B., Xu, H., Bader, G.D., Page, N., Robinson, M., Raghibizadeh, S., Hogue, C.W., Bussey, H., et al. (2001). Systematic genetic analysis with ordered arrays of yeast deletion mutants. Science *294*, 2364–2368.
Xu, Q., Johnston, G.C., and Singer, R.A. (1993). The Saccharomyces cerevisiae Cdc68 transcription activator is antagonized by San1, a protein implicated in transcriptional silencing. Mol. Cell Biol. *13*, 7553–7565.
Xu, Q., Singer, R.A., and Johnston, G.C. (1995). Sug1 modulates yeast transcription activation by Cdc68. Mol. Cell Biol. *15*, 6025–6035.

Supplemental Figure S1

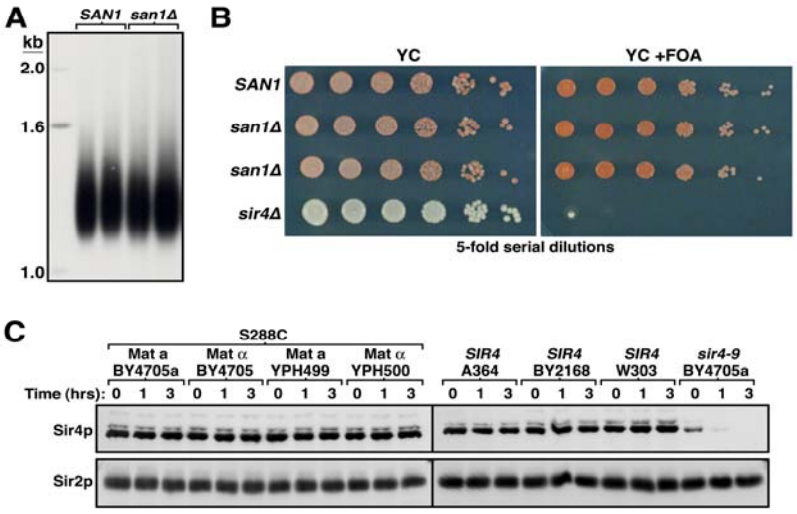

Figure S1. Loss of *SAN1* Has No Effect on Telomere Length or Silencing
(A) Genomic DNA from indicated strains was digested with XhoI, and the telomeres were visualized by Southern analysis using a probe directed against the subtelomeric Y' elements (Singer et al., 1998). Left lane is a DNA molecular weight ladder.
(B) Cells with *ADE2* and *URA3* telomeric reporter genes that are otherwise wild type (*SAN1, SIR4*), *san1*Δ or *sir4*Δ were grown in YEPD overnight at 30˚C to saturation. Five-fold dilutions of cells in distilled water were spotted onto YC plates, with or without 1mg/ml 5-FOA, and incubated at 30˚C for 3 days.
(C) Cycloheximide-chase assays of cells from the indicated strain were performed to assess the stability of wild-type Sir4p. Time after addition of cycloheximide is indicated above each lane. Images are of the same blot, sequentially probed with anti-Sir4p antibodies, and anti-Sir2p antibodies.

Table S1. List of Plasmids Used in This Study

Name	Features	Cloning Description	Reference
9Myc-CDC13	*9Myc-CDC13*, *TRP*, INT		(Qi and Zakian, 2000)
pBE3	*SAN1*, *URA3*, CEN		(Xu et al., 1993)
pLP0304	*SIR3*, *LEU2*, 2µ		(Stone et al., 2000)
pLP0791	*sir3-8*, *LEU2*, 2µ		(Stone et al., 2000)
pRG381	$P_{GAL1,10}$-*CDC34(C95S)*, *TRP1*, 2µ	1.2 kb XhoI-SpeI PCR fragment containing the *CDC34(C95S)* coding region was inserted between the XhoI-SpeI sites in pTCG	This study
pRG414	*CDC34*, *TRP1*, INT	1.55 kb SalI-PstI PCR fragment containing *CDC34* amplified from genomic DNA inserted between the SalI-PstI sites in pRS404	This study
pRG415	*SIR4*, *LEU2*, INT	6.1 kb NheI-ApaI fragment from pSIR4-ura3, containing the *SIR4* gene, was inserted into the XbaI-ApaI sites of pRS405. Contains unique XhoI-XbaI sites placed in front of the *SIR4* coding region.	This study
pRG418	*SIR3*, *LEU2*, INT	4.55 kb XbaI-HindIII fragment from pLP0304, containing the *SIR3* gene, was inserted between the XbaI-HindIII sites of pRS406.	This study
pRG419	*sir3-8*, *LEU2*, INT	4.55 kb XbaI-HindIII fragment from pLP0791, containing the *sir3-8* gene, was inserted between the XbaI-HindIII sites of pRS406.	This study
pRG424	*sir4-9*, *URA3*, CEN	Gap repair of MunI-digested pSIR4-URA3 in ste9-1 strains.	This study
pRG435	*SAN1*, *TRP1*, INT	3.5 kb BamHI-XhoI fragment from pBE3, containing the *SAN1* gene, inserted between the BamHI-XhoI sites of pRS404.	This study
pRG440	*sir4-9*, *LEU2*, INT	3.3 kb NheI-BsrGI fragment from pRG424, containing the *sir4-9* coding region, was used to replace the corresponding wild-type *SIR4* coding region in pRG415.	This study
pRG450	*SAN1*, *TRP1*, INT	1.3 kb PstI-XhoI PCR fragment, containing an insertion of BglII, NheI, SalI sites at the 3' end of	This study

		the *SAN1* gene, was used to replace the corresponding wild-type region in pRG435.	
pRG453	*GST-SAN1*	2.2 kb BamHI-EcoRI fragment from pRG449, containing the *SAN1* coding region, was inserted between the BamHI-EcoRI sites in pGEX-3X.	This study
pRG458	*san1*Δ*::KanMX*, INT	1.2 kb BsrGI-AatII PCR fragment, containing the KanMX cassette from pRS400, was used to replace the BsrGI-AatII *SAN1* region in pBE3.	This study
pRG459	*1Myc-SIR4*, *LEU2*, INT	2.2 kb NheI-BamHI PCR fragment, containing the single c-Myc epitope sequence NEQKLISEEDLFA in place of the wild-type *SIR4* coding sequence ^{371}SEQKMKEDADL, was used to replace the corresponding wild-type *SIR4* region in pRG415.	This study
pRG463	*sir4-9*, *LEU2*, INT	1.2 kb BamHI-BsrGI fragment from pRG440, containing the *sir4-9* coding region, was used to replace the corresponding wild-type *SIR4* region in pRG415.	This study
pRG465	*SAN1(C279S)*, *TRP1*, INT	300 bp ClaI-PstI PCR fragment, containing a C279S mutation in the *SIR4* coding region, was used to replace the corresponding wild-type *SAN1* sequences in pRG450.	This study
pRG466	*SAN1(C257S)*, *TRP1*, INT	300 bp ClaI-PstI PCR fragment, containing a C257S mutation in the *SIR4* coding region, was used to replace the corresponding wild-type *SAN1* sequences in pRG450.	This study
pRG472	*SAN1-3HSV*, *TRP1*, INT	A linker encoding the triple HSV epitope sequence, RSARQPELAPEDPEDIARQPELAPEDPEDIARQPELAPEDPEDIASPRVD, was inserted between the BglII-SalI sites at the 3' end of the *SAN1* gene in pRG450.	This study
pRG485	*GST-SAN1(C279S)*	500 bp ClaI-SacI fragment from pRG465, containing the C279S mutation, was used to replace the corresponding wild-type *SAN1* region in pRG453.	This study
pRG486	*GST-SAN1(C257S)*	500 bp ClaI-SacI fragment from pRG466, containing the C257S mutation, was used to replace the corresponding wild-type *SAN1* region in pRG453.	This study

pRG518	P_{TDH3}-*1Myc-SIR4*, *URA3*, INT	5.0 kb XhoI-SacI fragment from pRG459, containing the *1Myc-SIR4* coding region, was inserted between the SalI-SacI sites in pRH98-2.	This study
pRG524	*CDC13*, *URA3*, INT	1.3 kb XhoI-BamHI fragment from pSD252, containing 5' end of wild-type *CDC13,* was used to replace same fragment in pVL451.	This study
pRG526	*SAN1-GFP*, *TRP1*, INT	700 bp BglII-SalI PCR fragment, containing the GFP(F64L, S65T) coding region from EBO415, was added to the 3' end of *SAN1* by insertion between the BglII-SalI sites in pRG450.	This study
pRG531	P_{TDH3}-*1Myc-SIR4*, *LEU2*, INT	5.0 kb PstI-EagI fragment from pRG518, containing the *1Myc-SIR4* gene, was inserted between the PstI-EagI sites in pRS405.	This study
pRG539	P_{TDH3}-*1Myc-sir4-9*, *LEU2*, INT	4.6 kb AflII-BglII fragment from pRG531, containing *TDH3* promoter and 5' end of *1Myc-SIR4* coding region, was used to replace corresponding AflII-BglII fragment in pRG463.	This study
pRG562	$P_{GAL1,10}$-*UBC1(C88S)*, *TRP1*, 2µ	770 bp XhoI-SpeI PCR fragment containing the *UBC1(C88S)* coding region was inserted between the XhoI-SpeI sites in pTCG	This study
pRG563	*SAN1(-NLS)*, *TRP1*, INT	1.3 kb BsrGI-PstI PCR fragment, containing the K182C, R183S, K184A, R185T, K197S, K198Q, R199S mutations in the *SIR4* coding region, was used to replace the corresponding wild-type *SAN1* sequences in pRG450.	This study
pRG564	*GST-SAN1(-NLS)*	1.2 kb BspEI-SpeI fragment from pRG466, containing the -NLS mutations, was used to replace the corresponding wild-type *SAN1* region in pRG453.	This study
pRG573	*SAN1(C279S)-3HSV*, *TRP1*, INT	1.3 kb BsrGI-PstI fragment from pRG465, containing the C279S mutation, was used to replace wild-type region in *SAN1* in pRG472.	This study
pRG574	*SAN1(C257S)-HSV*, *TRP1*, INT	1.3 kb BsrGI-PstI fragment from pRG466, containing the C257S mutation, was used to replace wild-type region in *SAN1* in pRG472.	This study
pRG575	*SAN1(-NLS)-3HSV*, *TRP1*, INT	1.3 kb BsrGI-PstI fragment from pRG563, containing the -NLS mutations, was used to replace wild-type region in *SAN1* in pRG472.	This study

pRG606	*HA-cdc68-1*, *URA3*, INT	4.8 kb SacI-XbaI fragment from pXHA68-1, containing the *HA-cdc68-1* gene, was inserted between the SacI-XbaI sites in pRS406.	This study
pRG614	*HA-cdc68-1*, *URA3*, INT	1.56 kb BsrGI-NcoI fragment from pXHA68-1, containing the terminator sequence of *CDC68* and the 3' end of *URA3* but lacking the ClaI site, was used to replace the corresponding region within pRG606.	This study
pRG618	*cdc68-1*, *URA3*, INT	pRG614 digested with ClaI, then recircularized to remove the HA-tag coding sequence.	This study
pRG642	*9Myc-cdc13-1*, *TRP*, INT	3.6 kb SalI-EcoNI fragment from pVL451, containing the *cdc13-1* gene, was used to replace the corresponding 139 bp fragment from 9Myc-CDC13.	This study
pRG643	*9Myc-CDC13*, *TRP*, INT	3.6 kb SalI-EcoNI fragment from pRG524, containing the *CDC13* gene, was used to replace the corresponding 139 bp fragment from 9Myc-CDC13.	This study
pRG659	*1VSV-SIR3*, *LEU2*, INT	2.3 kb BlpI-NdeI PCR fragment, containing the single VSV epitope sequence YTDIEMNRLGK in place of the wild-type *SIR3* coding sequence ^{426}ETDNEMNGNGK, was used to replace the corresponding wild-type *SIR3* region in pRG418.	This study
pRG660	*1VSV-sir3-8*, *LEU2*, INT	2.3 kb BlpI-NdeI PCR fragment, containing the single VSV epitope sequence YTDIEMNRLGK in place of the wild-type *SIR3* coding sequence ^{426}ETDNEMNGNGK, was used to replace the corresponding wild-type *sir3-8* region in pRG419.	This study
pRG669	P_{TDH3}-*SIR3*, *LEU2*, INT	3.9 kb XbaI-Eco47III fragment from pRG659, containing the *1VSV-SIR3* coding region, was used to replace the *1Myc-SIR4* coding region in pRG531.	This study
pRG670	P_{TDH3}-*sir3-8*, *LEU2*, INT	3.9 Kb XbaI-Eco47III fragment from pRG660, containing the *1VSV-sir3-8* coding region, was used to replace the *1Myc-SIR4* coding region in pRG531.	This study
pRG674	*san1*Δ*::NatMX*, INT	1.2 kb BsrGI-AatII PCR fragment, containing the	This study

		NatMX cassette from pRS40Nat, was used to replace the BsrGI-AatII *SAN1* region in pBE3.	
pRG675	P_{TDH3}-*1Myc-sir4-9*, *URA3*, INT	5.8 kb XhoI-SacII fragment from pRG539, containing *TDH3* promoter and *1Myc-SIR4* coding region, was inserted between XhoI-SacII sites in pRS406.	This study
pRG689	*9Myc-cdc13-1*, *URA3*, INT	4.2 kb KpnI-SacI fragment from pRG642, containing the *9Myc-cdc13-1* gene, was inserted between the KpnI-SacI sites in pRS406.	This study
pRG772	$P_{GAL1,10}$-*UBC7(C89S)*, *TRP1*, 2µ	1.2 kb PstI-XbaI fragment from pRH1319 containing the *UBC7(C89S)* coding region was inserted between the PstI-SpeI sites in pTCG	This study
pRG775	*SAN1-3HSV-SV40NLS*, *TRP1*, INT	NheI-SalI linker containing the SV40 NLS sequence, SPKKKRKVEASGS, was inserted between the NheI-SalI sites at the end of *SAN1-3HSV* in pRG472.	This study
pRG779	*SAN1(-NLS)-3HSV-SV40NLS*, *TRP1*, INT	NheI-SalI linker containing the SV40 NLS sequence, SPKKKRKVEASGS, was inserted between the NheI-SalI sites at the end of *SAN1(-NLS)-3HSV* in pRG575.	This study
pRG782	*SAN1-3HSV-SV40NLS-GFP*, *TRP1*, INT	1.9 kb PflMI-BamHI fragment from pRG775, containing the *SAN1-3HSV-SV40NLS* coding region, was used to replace the corresponding region between the PflMI-BglI sites in pRG526.	This study
pRG810	$P_{GAL1,10}$-*RAD6(C88S)*, *TRP1*, 2µ	550 bp XhoI-SacI PCR fragment containing the *RAD6(C88S)* coding region was inserted between the XhoI-SacI sites in pTRP	This study
pRG813	*SAN1-3HSV-GFP*, *TRP1*, INT	1.1 kb NheI-EcoRI fragment from pRG782, containing the GFP(F64L, S65T) coding sequence, was used to replace the corresponding region in pRG472.	This study
pRG815	*SAN1(C279S)-3HSV-GFP*, *TRP1*, INT	1.1 kb NheI-EcoRI fragment from pRG782, containing the GFP(F64L, S65T) coding sequence, was used to replace the corresponding region in pRG573.	This study
pRG816	*SAN1(C257S)-3HSV-GFP*, *TRP1*, INT	1.1 kb NheI-EcoRI fragment from pRG782, containing the GFP(F64L, S65T) coding sequence, was used to replace the corresponding	This study

	INT	region in pRG574.	
pRG817	*SAN1(-NLS)-3HSV-GFP*, *TRP1*, INT	1.1 kb NheI-EcoRI fragment from pRG782, containing the GFP(F64L, S65T) coding sequence, was used to replace the corresponding region in pRG575.	This study
pRG818	*SAN1(-NLS)-3HSV-SV40NLS-GFP*, *TRP1*, INT	1.1 kb NheI-EcoRI fragment from pRG782, containing the GFP(F64L, S65T) coding sequence, was used to replace the corresponding region in pRG779.	This study
pRG830	*SAN1-3HSV-GFP*, *TRP1*, 2µ	4.3 kb BamHI-EcoRI fragment from pRG813, containing the *SAN1-3HSV-GFP* gene, was inserted between the BamHI-EcoRI sites in pRS424.	This study
pRG832	*SAN1(C257S)-3HSV-GFP*, *TRP1*, 2µ	4.3 kb BamHI-EcoRI fragment from pRG815, containing the *SAN1(C279S)-3HSV-GFP* gene, was inserted between the BamHI-EcoRI sites in pRS424.	This study
pRG833	*SAN1(C257S)-3HSV-GFP*, *TRP1*, 2µ	4.3 kb BamHI-EcoRI fragment from pRG816, containing the *SAN1(C257S)-3HSV-GFP* gene, was inserted between the BamHI-EcoRI sites in pRS424.	This study
pRG834	*SAN1(-NLS)-3HSV-GFP*, *TRP1*, 2µ	4.3 kb BamHI-EcoRI fragment from pRG817, containing the *SAN1(-NLS)-3HSV-GFP* gene, was inserted between the BamHI-EcoRI sites in pRS424.	This study
pRG835	*SAN1(-NLS)-3HSV-SV40NLS-GFP*, *TRP1*, 2µ	4.3 kb BamHI-EcoRI fragment from pRG818, containing the *SAN1(-NLS)-3HSV-SV40NLS-GFP* gene, was inserted between the BamHI-EcoRI sites in pRS424.	This study
pRH1255	*UBC1*		Randy Hampton
pRH1319	P_{TDH3}-*UBC7(C89S)*, *URA3*, INT		Randy Hampton
pRH990	P_{TDH3}-*3HA-Ub*, *URA3*, 2µ		Randy Hampton
pRS316	*URA3*, CEN		(Sikorski and Hieter, 1989)

pRS400	*KanMX*, INT		(Sikorski and Hieter, 1989)
pRS404	*TRP1*, INT		(Sikorski and Hieter, 1989)
pRS405	*LEU*, INT		(Sikorski and Hieter, 1989)
pRS406	*URA3*, INT		(Sikorski and Hieter, 1989)
pRS414	*TRP1*, CEN		(Sikorski and Hieter, 1989)
pRS424	*TRP1*, 2µ		(Sikorski and Hieter, 1989)
pSIR4-URA3	*URA3*, CEN	6.4 kb EcoRI/SalI fragment containing the *SIR4* gene inserted into the EcoRI/XhoI sites of pRS316.	This study
pTCG	$P_{GAL1,10}$, *TRP1*, 2µ		(Peterson et al., 2001)
pTRP	$P_{GAL1,10}$, *TRP1*, 2µ		(Singer and Gottschling, 1994)
pVL451	*cdc13-1*, *URA3*, INT		(Hughes et al., 2000)
pXHA68-1	*HA-cdc68-1*, *URA3*, YEp		(Xu et al., 1995)

Table S2. List of Yeast Strains Used in This Study

Name	Genotype	Source
BY4741	*MATa his3-1 leu2Δ0 met15Δ0 ura3Δ0*	(Brachmann et al., 1998)
JY128	*MATalpha ade2-101 hisΔ200 ura3-52 lys2-801 trp1Δ63*	
	leu2Δ1 ADE2::TEL-VR adh4::URA3::TEL-VIIL	Mark Hochstrasser
JY138	*MATalpha ade2-101 hisΔ200 ura3-52 lys2-801 trp1Δ63*	
	leu2Δ1 ADE2::TEL-VR adh4::URA3::TEL-VIIL cim3-1	Mark Hochstrasser
JY142	*MATalpha ade2-101 hisΔ200 ura3-52 lys2-801 trp1Δ63*	
	leu2Δ1 ADE2::TEL-VR adh4::URA3::TEL-VIIL cim5-1	Mark Hochstrasser
MHY501	*MATalpha his3Δ200 ura3-52 trp1-1 lys2-801 leu2-3,112*	Mark Hochstrasser
MHY624	*MATa his3Δ ura3-52 cdc34-2*	Mark Hochstrasser
RGY120	UCC7164 *sir4Δ::LYS2*	this study
RGY136	UCC725 *sir4::hphMX::SIR4::LEU2*	this study
RGY137	UCC725 *sir4::hphMX::sir4-9::LEU2*	this study
RGY139	UCC725 *sir4::hphMX::*P_{TDH3}*-1Myc-sir4-9::LEU2*	this study
RGY185	RGY137 *san1Δ::KanMX*	this study
RGY187	RGY139 *san1Δ::KanMX*	this study
RGY323	RGY139 pRH990 *(HA-Ub, URA3)*	this study
RGY324	RGY187 pRH990 *(HA-Ub, URA3)*	this study
RGY357	BY4741 *san1Δ::KanMX*	(Brachmann et al., 1998)
RGY371	UCC725 *sir4::hphMX::*P_{TDH3}*-1Myc-SIR4::LEU2*	this study
RGY373	RGY371 pRH990 *(HA-Ub, URA3)*	this study
RGY470	Y3656 *cdc68-1*	this study
RGY506	BY4741 *san1Δ::KanMX*	this study
RGY523	MHY501 *SIR4::URA3::*P_{TDH3}*-1Myc-sir4-9*	this study
RGY524	MHY624 *SIR4::URA3::*P_{TDH3}*-1Myc-sir4-9*	this study
RGY525	UCC725 *sir4::hphMX::*P_{TDH3}*-sir4-9::LEU2*	
	CDC13::TRP1::cdc13-1-9Myc	this study
RGY526	UCC725 *sir4::hphMX::*P_{TDH3}*-sir4-9::LEU2*	this study

	CDC13::TRP1::CDC13-9Myc	
RGY529	RGY525 *san1Δ::KanMX*	this study
RGY537	UCC3163 *sir3::HIS3::*P_{TDH3}*-1VSV-SIR3::LEU2*	this study
RGY538	UCC3163 *sir3::HIS3::*P_{TDH3}*-1VSV-sir3-8::LEU2*	this study
RGY560	RGY470 *san1Δ::KanMX*	this study
RGY593	RGY139 *pdr5Δ::NatMX*	this study
RGY595	RGY525 *pdr5Δ::NatMX*	this study
RGY606	RGY139 *CDC13::URA3::cdc13-1-9Myc*	this study
RGY607	RGY606 *san1Δ::KanMX*	this study
RGY608	RGY607 *san1Δ::KanMX::SAN1-3HSV::TRP1*	this study
RGY610	RGY607 *san1Δ::KanMX::SAN1(C279S)-3HSV:TRP1*	this study
RGY611	RGY607 *san1Δ::KanMX::SAN1(C257S)-3HSV:TRP1*	this study
RGY612	RGY607 *san1Δ::KanMX::SAN1(-NLS)-3HSV:TRP1*	this study
RGY614	RGY470 *pdr5Δ::NatMX*	this study
RGY649	RGY560 *trp1Δ::URA3*	this study
RGY650	RGY649 *san1Δ::KanMX::SAN1-3HSV::TRP1*	this study
RGY652	RGY649 *san1Δ::KanMX::SAN1(C279S)-3HSV:TRP1*	this study
RGY653	RGY649 *san1Δ::KanMX::SAN1(C257S)-3HSV:TRP1*	this study
RGY654	RGY649 *san1Δ::KanMX::SAN1(-NLS)-3HSV:TRP1*	this study
RGY672	JY128 *SIR4::LEU2::*P_{TDH3}*-1Myc-sir4-9*	this study
RGY673	JY138 *SIR4::LEU2::*P_{TDH3}*-1Myc-sir4-9*	this study
RGY674	JY142 *SIR4::LEU2::*P_{TDH3}*-1Myc-sir4-9*	this study
RGY743	RGY524 *trp1Δ::HIS3 cdc34-2::TRP1::CDC34*	this study
RGY745	RGY538 *san1Δ::NatMX*	this study
RGY851	RGY525 *ubc1Δ::KanMX*	this study
RGY852	RGY525 *ubc4Δ::KanMX*	this study
RGY853	RGY525 *ubc5Δ::KanMX*	this study
RGY855	RGY525 *ubc6Δ::KanMX*	this study
RGY857	RGY525 *ubc7Δ::KanMX*	this study

RGY859	RGY525 *ubc8Δ::KanMX*	this study
RGY861	RGY525 *ubc10Δ::KanMX*	this study
RGY863	RGY525 *ubc11Δ::KanMX*	this study
RGY867	RGY525 *ubc13Δ::KanMX*	this study
RGY915	RGY606 pRG381 ($P_{GAL1,10}$-*CDC34(C95S), TRP1*, 2µ)	this study
RGY916	RGY606 pRG562 ($P_{GAL1,10}$-*UBC1(C88S), TRP1*, 2µ)	this study
RGY917	RGY606 pRG772 ($P_{GAL1,10}$-*UBC7 (C89S), TRP1*, 2µ)	this study
RGY918	RGY606 pRG810 ($P_{GAL1,10}$-*RAD6(C88S), TRP1*, 2µ)	this study
RGY963	UCC7164 *san1Δ::KanMX*	this study
RGY968	RGY607 *san1Δ::KanMX::SAN1(-NLS)-3HSV-SV40NLS::TRP1*	this study
RGY970	RGY649 *san1Δ::KanMX::SAN1(-NLS)-3HSV-SV40NLS::TRP1*	this study
RGY974	RGY470 *trp1Δ::URA3*	this study
RGY975	RGY525 *rad6Δ::KanMX*	this study
RGY983	RGY974 pRG381 ($P_{GAL1,10}$-*CDC34(C95S), TRP1*, 2µ)	this study
RGY984	RGY974 pRG562 ($P_{GAL1,10}$-*UBC1(C88S), TRP1*, 2µ)	this study
RGY985	RGY974 pRG772 ($P_{GAL1,10}$-*UBC7 (C89S), TRP1*, 2µ)	this study
RGY986	RGY974 pRG810 ($P_{GAL1,10}$-*RAD6(C88S), TRP1*, 2µ)	this study
RGY987	RGY187 *san1Δ::KanMX::SAN1-3HSV-GFP::TRP1*	this study
RGY989	RGY187 *san1Δ::KanMX::SAN1(C279S)-3HSV-GFP::TRP1*	this study
RGY990	RGY187 *san1Δ::KanMX::SAN1(C257S)-3HSV-GFP::TRP1*	this study
RGY991	RGY187 *san1Δ::KanMX::SAN1(-NLS)-3HSV-GFP::TRP1*	this study
RGY992	RGY187 *san1Δ::KanMX::SAN1(-NLS)-3HSV-SV40NLS-GFP::TRP1*	this study
RGY993	RGY187 pRG830 (*SAN1-3HSV-GFP, TRP1*, 2µ)	this study
RGY995	RGY187 pRG832 (*SAN1(C279S)-3HSV-GFP, TRP1*, 2µ)	this study
RGY996	RGY187 pRG833 (*SAN1(C257S)-3HSV-GFP, TRP1*, 2µ)	this study
RGY997	RGY187 pRG834 (*SAN1(-NLS)-3HSV-GFP, TRP1*, 2µ)	this study

RGY998	RGY187 pRG835 (*SAN1(-NLS)-3HSV-SV40NLS-GFP, TRP1*, 2μ)	this study
UCC3163	*MATa ura3-52 his3-11 leu2 trp1Δ ade2Δ::hisG can1Δ::hisG ADE2::TEL-VR adh4::URA3::TRP1::TEL-VIIL sir3::HIS3*	this study
UCC7164	*MATa ade2Δ::hisG met15Δ0 his3Δ200 ura3Δ0 trp1Δ63 lys2Δ0 leu2Δ0 ADE2::TEL-VR adh4::URA3::TEL-VIIL*	this study
UCC725	*MATa ade2Δ::hisG his3Δ200 leu2Δ0 lys2Δ0 met15Δ0 trp1Δ63 ura3Δ0 ADE2::TEL-VR sir4::hphMX*	this study
Y3656	*MATalpha met15Δ0 his3Δ0 ura3Δ0 lys2Δ0 leu2Δ0 can1Δ::P_{MFA1}-HIS3-P_{MFa1}-LEU2*	(Tong et al., 2001)